

Toward a Unified Approach to Torsion-Shear Constraints in Convex Limit Analysis of Masonry

Elham Mousavian(✉)

Edinburgh School of Architecture and Landscape Architecture (ESALA), Edinburgh College of Art, The University of Edinburgh, 20 Chambers Street, Edinburgh EH1 1JZ, UK
emousavi@ed.ac.uk

Abstract. Limit analysis of discrete masonry assemblies, developed from Hyman's theorem, has proven to be an effective and computationally efficient approach for analyzing masonry structures. The convex method builds on this by abstracting the interface between two rigid blocks to a single point—typically the centroid—where internal forces and moments are computed to equilibrate external loads applied to the blocks. These internal actions are constrained to prevent different types of failure, including torsion-shear failure, which defines the maximum combined tangential force and torsional moment an interface can resist. Several studies based on the convex method have formulated torsion-shear constraints, though all are limited to rectangular interfaces. Those formulations address both dry frictional contacts between blocks and cohesive interfaces within blocks, where failure can occur due to finite tensile and shear strength. In both cases, the torsion-shear constraint is highly sensitive to the geometry of the interface. To overcome this, researchers have proposed general approximation methods for torsion-shear constraints that apply across rectangular interfaces with varying aspect ratios. This paper, for the first time, explores the extension of the convex method—specifically its torsion-shear constraints—to arbitrary planar interfaces bounded by convex closed polylines. It investigates whether a single approximate constraint can be established to cover diverse geometries. The proposed formulation includes both zero-tension frictional interfaces and internal discontinuities with finite shear and tensile strength. Given the proven accuracy and efficiency of the convex method, this work represents a key step toward its application in complex assemblies with diverse interface geometries.

Keywords: Torsion-shear yield function · arbitrary planar interfaces · dry and cohesive interfaces · discrete assemblies

1 Introduction

The limit analysis of rigid blocks, as formulated by Heyman [1], is based on modeling a masonry discrete structure as an assembly of rigid blocks. In this approach, external forces applied to the structure are balanced by internal stresses distributed along the interfaces between the blocks. When these stresses exceed their limits, failure occurs at the corresponding interfaces.

© The Author(s), under exclusive license to Springer Nature Switzerland AG 2026
O. Gervasi et al. (Eds.): ICCSA 2025 Workshops, LNCS 15886, pp. 289–301, 2026.
https://doi.org/10.1007/978-3-031-97576-9_19

Adopting this theorem, an abstraction method introduced by Livesley [2] that first represents an interface between rigid blocks as one or more 'contact points' distributed along the surface and then computes the internal forces at these points to balance the external forces. Two major models extending this approach are known as the convex and concave models [3].

The convex model simplifies an interface to a single representative point and seeks to determine the internal normal and tangential forces, along with bending (flexural) and torsional moments, to characterize the interface behavior [3]. In contrast, the concave model represents the interface using multiple points and calculates the internal normal and tangential forces at each point to maintain equilibrium with the external forces. Similar to the convex model, these forces are subject to constraints, and when these constraints are reached, the interface reaches its limit state before failure occurs [2].

The evolution of constraints in both the convex and concave approaches will be discussed in more detail below. However, as a general observation, the convex approach has proven capable of producing more accurate results, whereas the concave approach offers greater flexibility in modeling assemblies with complex block geometries and, consequently, more varied interface configurations. In other words, while the convex model has primarily been applied to assemblies with rectangular interfaces, the concave model has been explored for interfaces with a wide range of polygonal boundaries as well as linear or nonlinear surfaces [4, 5]—albeit with an expected reduction in accuracy.

This reduction in accuracy is particularly evident in the shear-torsion capacity of the interface, which reflects the resistance of an interface under a combination of tangential force and torsional moment. Casapulla and Maione [3] demonstrated that the torsion-shear capacity predicted by the concave model is significantly higher than the experimental results. In the case of pure torsion, the estimated capacity can reach about 1.8 times the actual torsional strength of a rectangular interface with a width-to-length ratio of 1.5. In contrast, the same study showed that the convex model provides a much closer match to experimental data for the same interface geometry.

Given this observed accuracy—particularly in simulating torsion-shear constraints—this paper explores the potential extension of the convex model to non-rectangular planar interfaces. This approach can lead to more accurate form-finding and the innovative design of a new generation of stone assemblies characterized by non-rectilinear geometries. The reintroduction of stone construction has been strongly advocated in [6–9], and exhibitions like [10] and [11], who refers to this shift as a "New Stone Age." This resurgence is largely driven by global concerns over embodied carbon and resource depletion, which have prompted a renewed interest in natural materials requiring minimal processing compared to industrialized materials. Among both organic and inorganic natural materials, stone and other earth-derived substances hold particular promise. Unlike organic materials such as wood and bamboo, stone and other earth-born materials typically involve lower embodied water and have a reduced environmental impact on forests and vegetation. To support the revival of geo-sourced material construction—an approach increasingly pursued in manufacturing and building practices as highlighted by [11, 12]—it is essential to develop advanced computational tools and numerical models for early-stage form-finding. These tools are critical for exploring structurally optimized geometries, ensuring both precision in design and computational efficiency.

As will be shown later, the torsion-shear yield surface exhibits a high degree of non-linearity, strongly influenced by the geometry of the interface. This paper investigates a simplified linearized method that is both extendable and applicable to a wide range of arbitrary planar interface geometries.

In the remainder of the introduction, a review of the development and evolution of the constraints—including torsion-shear—governing internal forces in both the convex and concave models will be presented, as discussed in various studies. The constraints should be defined based on the expected behavior at the interface between rigid bodies. Traditionally, failure discontinuity from which a discerte assembly can fail was considered the dry (mortar less) interfaces between the rigid block. Such interfaces are typically considered fully plastic [13], carrying no tensile strength, while their tangential behavior is governed by frictional resistance along the interface. This abstraction model was later extended to account for cohesive (inner) interfaces within blocks—interfaces along which block fracture may occur—alongside the dry interfaces between blocks, forming what is known as a multi-surface plasticity approach [13]. Portioli et al. [14] developed a method in which both inner and dry interfaces were modeled as plastic, differing primarily in their tangential cohesion. Mousavian et al. [15] and Iannuzzo et al. [16] proposed a convex model in which dry and inner interfaces follow distinct failure criteria: while dry interfaces are frictional, following Coulomb's law and carrying no tensile forces, inner interfaces can carry tension, and their tangential behavior is governed by the material's shear strength. Yet, the behaviour of both inner and dry faces have been considered plastic. To the best knowledge of the author, the only work that has attempted to incorporate combinations of different elasto-plastic failure modes at the interfaces is [17], though this approach has so far been limited to 2D cases.

Considering purely plastic behaviour at an interface means to prevent flexural hinges at a face with zero tensile strength, it must be ensured that, in the convex model, the internal normal force remains within the interface boundary. Instead in the concave model, the internal normal force at each point cannot be negative, as a negative value would indicate tensile forces.

Defining constraints that govern tangential failure at an interface is inherently more complex. Tangential failure can take several forms: pure shear, where the interface is subjected solely to a tangential force acting at the centroid; pure torsion, where only a torsional moment is applied at the interface centroid; torsion-shear, where the entire interface is subjected to both a tangential force and a torsional moment; and finally, torsion-shear-flexure interaction, which arises when the normal force is not applied at the centroid—resulting in a non-uniform normal stress distribution across the interface. In this latter case, it is assumed that the normal force is uniformly distributed only over a portion of the interface, known as the effective area [13], while the remaining part of the interface carries no normal force. The torsion-shear interaction is then considered to occur within this effective area.

In the concave model for a frictional (dry) interface, representing all types of tangential failure listed above requires assuming that the ratio between the tangential and normal force at each contact point does not exceed the friction coefficient [18]. For an inner interface, however, the tangential force must not exceed a certain proportion of the total shear resistance, which is determined by multiplying the material's shear

strength by the interface area [19]. The resulting constraints are highly dependent on the number and placement of contact points on the interface. For example, Casapulla and Maione [3] demonstrated that when contact points are positioned at the corners of a rectangular interface, the computed torsion-shear and torsion-shear-flexural resistance is overestimated up to close two times compared to actual experimental results. They suggest shifting the contact points inward from the boundary using a specific formula, in order to obtain a more realistic estimate of the interface resistance. However, this solution mainly improves torsion-shear accuracy. Shifting contact points inward leads to underestimating bending capacity, since in plastic behavior, rotational hinges form at the boundary where eccentric normal forces act—suggesting contact points are better placed along the edges. Mousavian and Casapulla [19] and Casapulla et al. [20] investigated different numbers and placements of contact points on a rectangular inner face to determine the most accurate shear-torsion resistance. However, the question remains open, as the ideal number and positioning of contact points vary depending on the interface geometry.

In contrast, the convex model calculates the torsion-shear resistance of the interface by summing the torsional resistance at each point on the interface. Adopting the method proposed by Casapulla and Portioli [21], this approach will be detailed in Sect. 2. The torsion-shear yield graph for rectangular interfaces exhibits a high degree of non-linearity yet consistently maintains a convex shape, though the degree of convexity varies depending on the width-to-length ratio (see Sect. 2 for further details). Ultimately, the final results demonstrate the highest compatibility with experimental tests for both dry and inner interfaces [3, 20], leading to the conclusion that the convex model provides more accurate results than the concave model when the contact points in the concave model are placed at the corners of the interface boundary.

As mentioned above, the torsion-shear yield surface is highly non-linear, with this non-linearity strongly influenced by the aspect ratio of the rectangular interface. Orduña and Lourenço [13], Casapulla and Portioli [21], and Portioli et al. [22] investigated a wide range of aspect ratios from zero to infinite values to determine upper and lower bounds for the torsion-shear yield surface and proposed various linearized approximations, independent of aspect ratio. These approximations will be introduced in the Sect. 3.

Building on the reasoning behind these approximations, this paper explores whether a generalized linear approximation can be developed—one that is valid not only for rectangular interfaces but also for arbitrary planar geometries. Section 2 presents the method for determining the actual torsion-shear yield surface for any arbitrary geometry. Section 3 reviews existing linearization methods and examines whether a general approximation can be applied across different interface shapes. Section 4 concludes the findings.

2 Torsion-Shear Yield Function

The convex method of limit analysis is based on abstracting the interface between two blocks to a single point—typically the interface centroid—and computing the internal forces, bending moments, and torsional moment at that point to equilibrate the external

forces applied to the block's centroid [3]. These internal components include a normal force N, two orthogonal tangential forces (T_u and T_v), two corresponding bending moments M_u and M_v (whose axis of moment is parallel to T_v and T_u, respectively), and a torsional moment M_t whose axis of moment is aligned with the normal vector N.

For an arbitrary interface $\boldsymbol{\varsigma}$ with boundary $\boldsymbol{\beta}$, when no bending moment is applied at the centroid, the entire interface is uniformly compressed, meaning the full surface engages in plastic tangential interaction. In this case, if only a tangential force T_v acts at the centroid, the interface experiences pure shear along the V direction. Assuming the maximum tangential stress that can be imposed on an arbitrary point **P** of the interface is denoted by τ_0, in the pure shear case all τ_0 vectors are parallel and aligned with the v direction (see Fig. 1), the maximum allowable tangential force in the V direction, referred to as $T_{v0\text{-pure shear}}$, is equal to:

$$T_{v0-pureshear} = \tau_0 \int_{u_{min}}^{u_{max}} du \int_{b(u)}^{t(u)} dv \tag{1}$$

This double integral equation involves integrating a function of two variables (u and v) in two steps: first integration is done with respect to v, while u is treated as constant (e.g., u_1) (Fig. 1). For this, the bottom and top points on the interface boundary corresponding to $u = u_1$ are identified, and the moment of τ_0 about the centroid is integrated at all points between these two points.

To determine the bottom and top points for a given u, the interface boundary is divided into two functions, **b(u)** and **t(u)**. If the boundary is curved, it should first be simplified into a piecewise polyline. Then, the points with minimum and maximum u values (u_{min} *and* u_{max}) are located, and the boundary is split into two open polylines. Each polyline is defined as a piecewise linear function—**b(u)** and **t(u)**—composed of linear segments over specific intervals (Fig. 1). For any u between u_{min} and u_{max}, the corresponding v on **b(u)** and **t(u)** can be found.

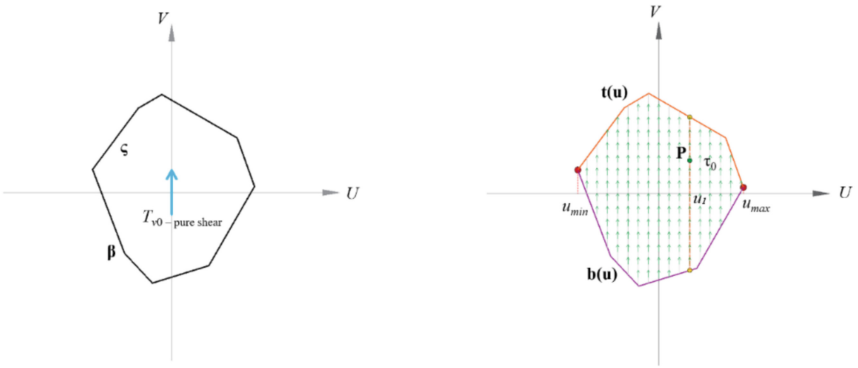

Fig. 1. Pure shear modelling of an arbitrary interface.

After the first integration, the result is integrated with respect to u, from u_{min} to u_{max}. In fact, in the simple case of pure torsion along the V direction, this double integral

simplifies to the interface area. Evidently, when both T_u and T_v act at the centroid, the interface experiences pure shear inclined with respect to the U axis, forming an angle of $\alpha = arctan\ (T_v\ /\ T_u)$. In this case, maximum value of T_u and T_v, i.e., $T_{u0\text{-pure shear}}$ and $T_{v0\text{-pure shear}}$ are simply equal to:

$$T_{u0-pureshear} = T_{0-pureshear}.\cos(\alpha) \tag{2}$$

$$T_{v0-pureshear} = T_{0-pureshear}.\sin(\alpha) \tag{3}$$

On the other hand, when only a torsional moment is acting at the centroid—known as pure torsion interaction—the maximum value M_t can take, denoted as M_{T0}, corresponds to the stress distribution pattern depicted in Fig. 2, in which τ_0 is tangential to a circle centered at the centroid of rotation, which in this case coincides with the interface centroid. Extending the formulation developed by Casapulla and Portioli [21], $M_{T0\text{-pure torsion}}$ can be found as:

$$M_{T0-puretorsion} = \tau_0 \int_{u_{min}}^{u_{max}} du \int_{b(u)}^{t(u)} \sqrt{u^2 + v^2} dv \tag{4}$$

In this formula, the centroid is considered the origin of a local coordinate system whose axes are U and V.

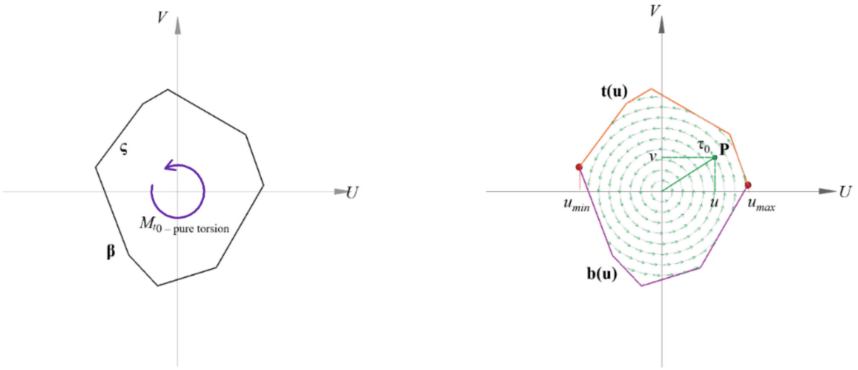

Fig. 2. Pure torsion modelling of an arbitrary interface.

When T_u and T_v act in combination with a torsional moment M_t at the centroid, the circular stress distribution pattern observed in pure torsion remains the same; however, the center of these circles—known as the center of rotation—shifts away from the interface centroid, as shown in Fig. 3. In this case, the maximum possible T_u and T_v denoted as T_{u0} and T_{v0} are equal:

$$T_{v0} = \tau_0 \int_{u_{min}}^{u_{max}} du \int_{b(u)}^{t(u)} \frac{u}{\sqrt{u^2 + v^2}} dv \tag{5}$$

$$T_{u0} = \tau_0 \int_{u_{min}}^{u_{max}} du \int_{b(u)}^{t(u)} \frac{v}{\sqrt{u^2 + v^2}} dv \tag{6}$$

And the moment acting on the center of rotation which is in fact equal to $M_{t0} + T_{u0}.\ s_v + T_{v0}.\ s_u$ can be given by:

$$M_{t0} + T_{u0}.s_v + T_{v0}.s_u = \tau_0 \int_{u_{min}}^{u_{max}} du \int_{b(u)}^{t(u)} \sqrt{u^2 + v^2} dv \tag{7}$$

where s_u and s_v are distances of the center of mass and the interface centroid in the U and V directions, respectively.

τ_0, introduced as the maximum tangential stress that can be sustained at any point of an interface, is defined differently depending on the interface type. For dry interfaces, τ_0 is equal to $\mu \cdot n$, where n is the normal stress uniformly distributed over the interface (i.e., $n = N / A$, with A being the interface area). For inner (cohesive) interfaces, τ_0 corresponds to the material's shear strength.

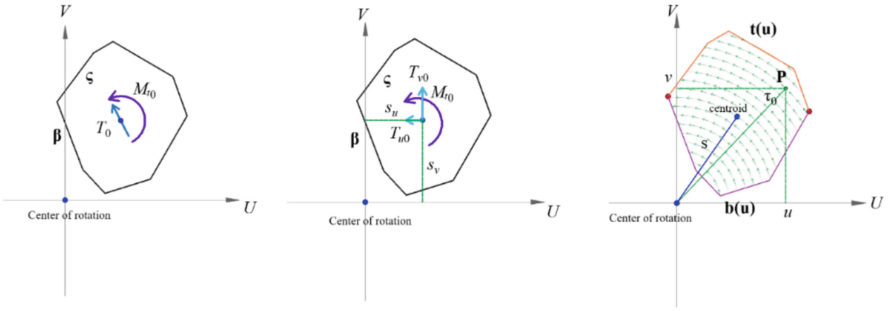

Fig. 3. Combined torsion-shear interaction of an arbitrary interface.

A visual representation of Eq. 7—which defines the torsion-shear yield curves—is provided in Fig. 4. It illustrates two cases: (1) a rectangular dry interface between two blocks (30 × 20 cm) with a normal force N of 467 N acting at the interface centroid, and a friction coefficient $\mu = 0.64$; and (2) a rectangular inner interface within a block (10 × 3 cm) with a shear strength of 0.08 kN/m, both subjected to combined T_v and M_t. These two graphs were produced by the author and are fully detailed in [3, 20].

These two graphs are concave downward and decreasing. As shown by Orduña and Lourenço [13], Casapulla and Maione [3], for any aspect ratio—from zero to infinity—of a rectangular interface, the yield curve maintains the same general shape, although its degree of convexity varies with the aspect ratio. Based on this observation, several approximation methods have been proposed [13, 21, 22], which will be discussed in the next section.

3 Torsion-Shear Yield Function Approximation

By obtaining the torsion-shear yield curves for a wide range of rectangular interfaces with aspect ratios from zero to infinity, Orduña and Lourenço [13], Casapulla and Portioli [21], and Portioli et al. [22] developed three different approximation methods. These approximations are essential, as the high degree of non-linearity in the exact yield curves unnecessarily complicates both the expressions and the computational effort.

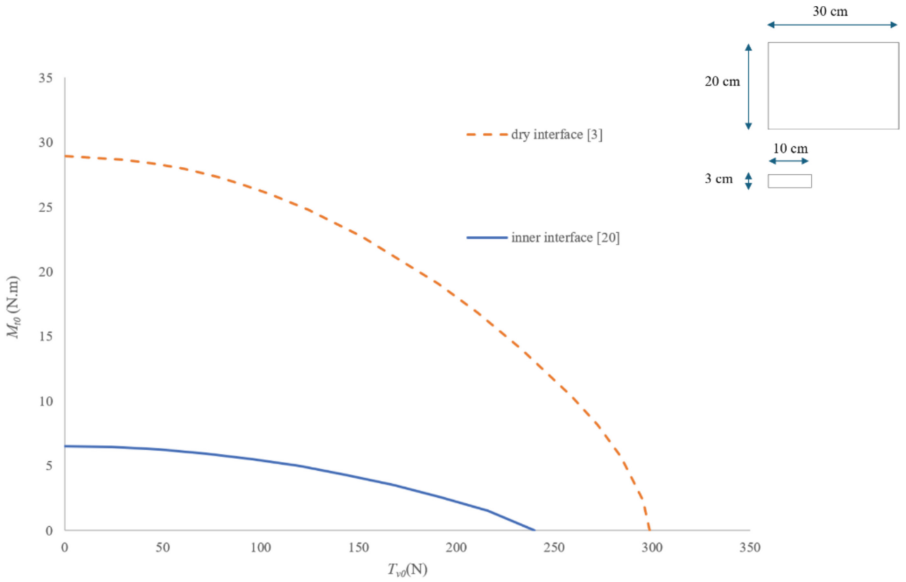

Fig. 4. Torsion-shear yield curve for a dry and an inner cohesive rectangular face.

Orduña and Lourenço [13] proposed a piecewise approximation consisting of three segments: a horizontal segment with $M_{t0} = M_{t0\text{-}pure\ torsion}$, an inclined middle section, and a vertical line with $T_0 = T_{0\text{-}pure\ shear}$ (Fig. 5). This piecewise graph is based on the average shape of yield curves across the full range of aspect ratios between zero and infinity, as their influence was found to be relatively minor.

In contrast, Casapulla and Portioli [21] aimed to develop an approximation based on the minimum envelope of all possible yield curves, ensuring that the torsion-shear resistance of any rectangular interface remains above this lower bound. They observed that the yield curves of rectangular interfaces always lie above a parabolic shape, which they adopted as the lower-bound curve. This was then linearized into a two-piece approximation (see Fig. 5).

The simplest yet effective approach is a straight-line approximation connecting the two extremes—pure torsion and pure shear (Fig. 5). This function in case T_v and M_t are acting on the interface centroid can be written as:

$$\frac{M_{t0}}{M_{t0-puretorsion}} + \frac{T_{v0}}{T_{v0-pureshear}} = 1 \tag{8}$$

This method, also based on the minimum curve principle, was adopted by Portioli et al. [22] and validated through application to various configurations, including single brick wall panels, corner panels, and U-shaped brick wall assemblies. The results confirmed its effectiveness for practical masonry analysis.

Adopting the last linear approximation concept (Eq. 8), this paper investigates whether the approach can be extended to arbitrary interface geometries. Based on the principle of constructing a minimum curve, it must first be established whether the

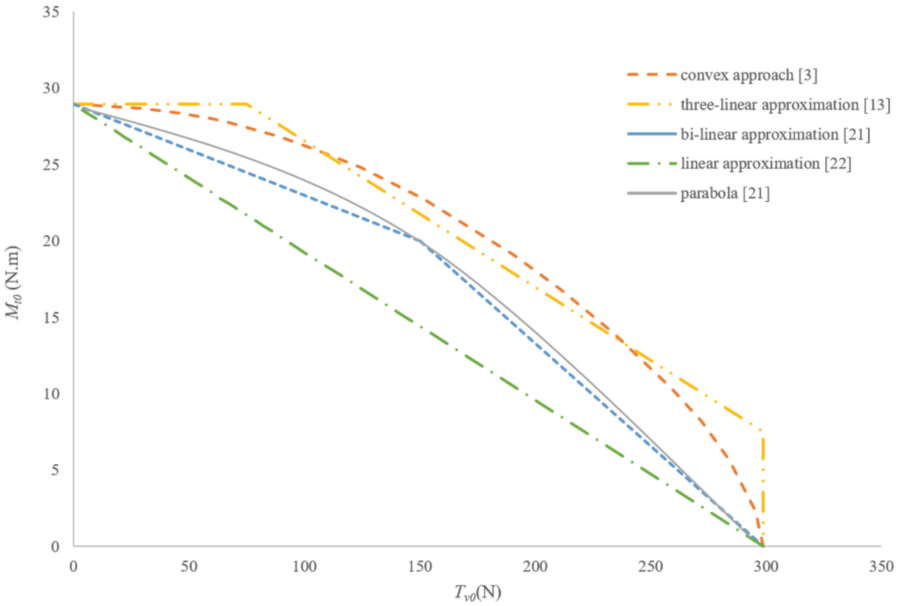

Fig. 5. Various approximations of torsion-shear yield curve.

torsion-shear yield curve (with endpoints corresponding to the maximum pure torsion and pure shear capacities—computed by Eqs. 1 and 2, respectively) is always concave downward, descending. In other words, it must be verified that the torsion-shear curve does not take on a different shape, such as a concave upward or non-monotonic form. If such cases exist, a linear approximation connecting the extremes of pure shear and pure torsion would no longer be valid. If not, this linear approximation can be confidently assumed as a lower bound that the torsion-shear yield curve can never fall below.

To this aim, this paper tracks the geometric variations along the graph, which by convention starts from the left (starting point corresponding to the pure torsion case) and ends on the right (ending point corresponding to the pure shear case).

In the case where T_v and M_t act on the interface centroid, with $M_t = T_v \cdot ecc$, where ecc represents the eccentricity along the U direction from the centroid, the variation along the torsion-shear yield curve—from left to right—can be analogized to the change in ecc. At the leftmost point of the curve (representing pure torsion), ecc is close to infinite. Moving rightward along the curve corresponds to a gradual decrease in ecc, approaching zero at the rightmost point (representing pure shear).

Similarly, this analogy can be extended to the distance between the center of rotation and the interface centroid, s_u. At the leftmost point of the curve, s_u is zero; as we move toward the right, s_u increases, becoming nearly infinite in the pure shear case (see Fig. 6).

In this case, where T_v and M_t act on the interface centroid, Eq. 7 can be rewritten as:

$$M_{t0} = -s_u.T_{v0} + \tau_0 \int_{u_{min}}^{u_{max}} du \int_{b(u)}^{t(u)} \sqrt{u^2 + v^2} dv \tag{9}$$

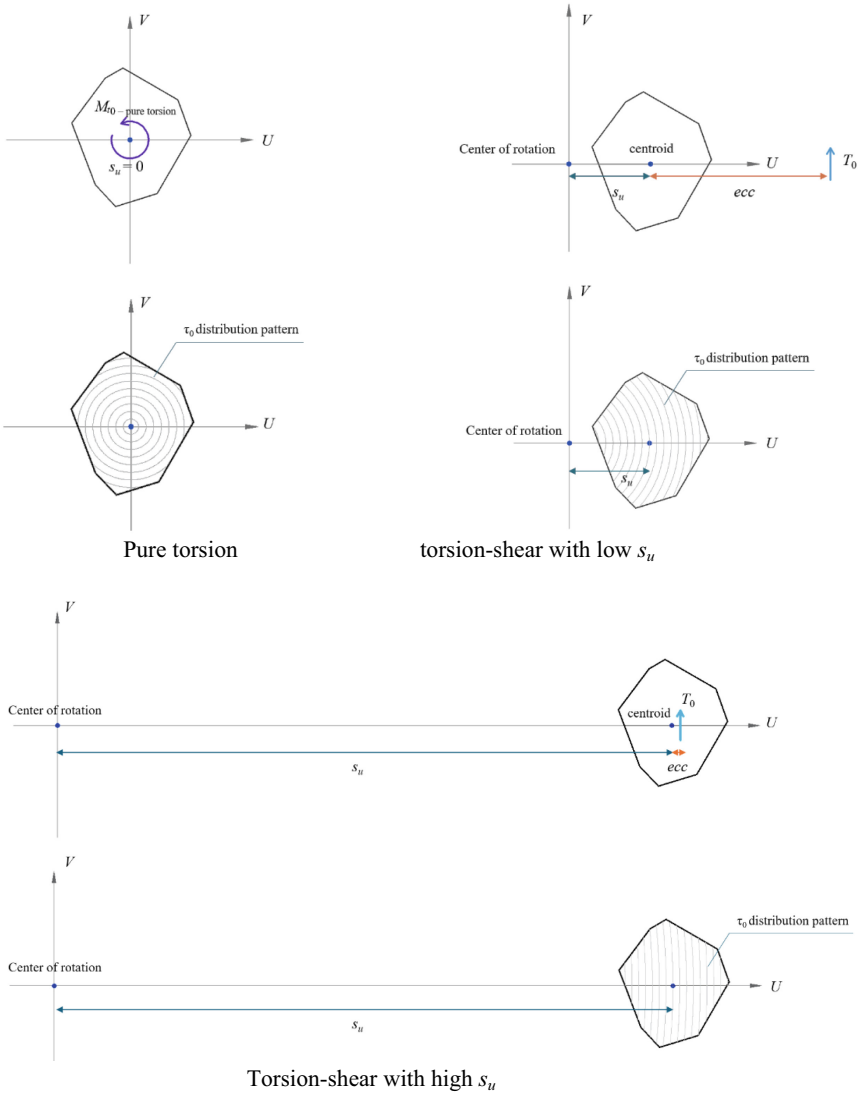

Fig. 6. Stress distribution pattern for various distance between the center of rotation and the interface centroid.

For the torsion-shear yield curve, -s_u in this equation can be interpreted as the slope of the curve. As mentioned above, moving from left to right along the curve, this slope increases from zero to near infinity. This observation directly supports the conclusion that the torsion-shear yield curve is always concave downward and decreasing. Looking more closely, we can also see that in the case of pure torsion—when the expression $-s_u.T_{v0}$ equals zero—Eq. 9 reduces to Eq. 2. Similarly, in the case of pure shear, Eq. 9

can be rewritten as:

$$T_{v0} = \tau_0 \frac{\int_{u_{min}}^{u_{max}} du \int_{b(u)}^{t(u)} \sqrt{u^2 + v^2} dv}{s_u} = \tau_0 \int_{u_{min}}^{u_{max}} du \int_{b(u)}^{t(u)} \frac{\sqrt{u^2 + v^2}}{s_u} dv \tag{10}$$

Since the center of rotation is assumed to be very far from the interface in the case of pure shear, the stress distribution lines become almost parallel. As a result, the term $\frac{\sqrt{u^2+v^2}}{s_u}$ can be approximated as 1, and the equation simplifies to:

$$T_{v0} = \tau_0 \int_{u_{min}}^{u_{max}} du \int_{b(u)}^{t(u)} dv \tag{11}$$

Which is a double integral equal to the interface area, as observed in Eq. 1.

This clearly shows that the torsion-shear yield surface for any arbitrary planar interface with a convex boundary is concave downward and descending, with two extremes corresponding to pure torsion and pure shear. Therefore, the linear constraint proposed by Portioli et al. [22] (Eq. 8) can be considered a valid approximation, enabling us to extend the convex method to any arbitrary block—and consequently, any interface geometry—when this approximation is incorporated.

4 Conclusions and Future Works

This paper investigated whether a unique approximation can be found to serve as the torsion-shear yield function for any arbitrary planar interface with a convex boundary. A general method was first presented to analyze the actual torsion-shear behavior at such interfaces. Given the high degree of non-linearity in the torsion-shear yield function, the paper then explored whether a simplified approximation can be valid across all possible interface geometries between blocks. This investigation is based on determining whether the yield curve can ever take a form that is not concave downward and decreasing. By demonstrating that such a case is not possible, the paper proposed using a linear yield function—bounded by the two extremes of pure shear and pure torsion—as a general approximation. This enables the extension of the convex method to analyze complex masonry assemblies with arbitrary block and interface geometries.

While the proposed linear torsion-shear approximation was guaranteed to serve as a lower bound, the degree of underestimation—depending on the actual convexity of the yield function—requires further investigation. Also, this paper did not address the combined torsion-shear-flexure interaction at the interface, where the primary challenge lies in determining the effective area for interfaces of arbitrary geometry.

Disclosure of Interests. The author has no competing interests to declare that are relevant to the content of this article.

References

1. Heyman, J.: The stone skeleton. Int. J. Solids Struct. **2**(2), 249–279 (1966)
2. Livesley, R.K.: A computational model for the limit analysis of three-dimensional masonry structures. Meccanica **27**, 161–172 (1992)
3. Casapulla, C., Maione, A.: Modelling the dry-contact interface of rigid blocks under torsion and combined loadings: Concavity vs. convexity formulation. Int. J. Non-Linear Mech. **99**, 86–96 (2018)
4. Frick, U., Van Mele, T., Block P.: Decomposing three-dimensional shapes into self-supporting, discrete-element assemblies. In: Modelling Behaviour: Design Modelling Symposium 2015, pp. 187–201. Springer International Publishing (2015)
5. Kao, G.T-C., Iannuzzo, A., Thomaszewski, B., Coros, B., Van Mele, T., Block, P.: Coupled rigid-block analysis: stability-aware design of complex discrete-element assemblies. Computer-Aided Design **146** (2022)
6. Boote, S., Lynes, A.: Stone as a structural material, Part 1: Mechanical properties. The Physics Teacher **98**(3), 20–25 (2020)
7. Boote, S.: Stone as a structural material, Part 2: Traditional and reinforced stone stairs. Struct. Eng. **98**(6), 18–23 (2020)
8. Boote, S., Lynes, A.: Stone as a structural material, Part 3: Posttensioned stone structures. Struct. Eng. **98**(8), 22–28 (2020)
9. Boote, S.: Stone as a structural material, Part 4: Contemporary loadbearing stone buildings. Struct. Eng. **98**(10), 28–33 (2020)
10. AAU Anastas: Official Website, https://www.aauanastas.com/, last accessed 2025/05/08
11. Webb Yates Engineers: The New Stone Age, https://webbyates.com/projects/the-new-stone-age/, last accessed 2025/05/08
12. Dezeen: Tavs Jorgensen develops cob bricks for low-carbon construction. Dezeen, https://www.dezeen.com/2024/10/29/tavs-jorgensen-cob-bricks-low-carbon/, last accessed 2025/05/08
13. Orduña, A., Lourenço, P.B.: Three-dimensional limit analysis of rigid blocks assemblages, Part I: Torsion failure on frictional interfaces and limit analysis formulation. Int. J. Solids Struct. **42**, 5140–5160 (2005)
14. Portioli, F., Cascini, L., Casapulla, C., D'Aniello, M.: Limit analysis of masonry walls by rigid block modelling with cracking units and cohesive joints using linear programming. Eng. Struct. **57**, 232–247 (2013)
15. Mousavian, E., Kibriya, G., Bagi, K., Iannuzzo, A.: multi-surface plasticity model for analysis of complex interlocking assemblies, In: 6th International Conference on Structures and Architecture, Antwerp, Belgium (2025)
16. Iannuzzo, A., Herczeg, M. Bagi, K., Mousavian, E.: Equilibrium analysis of 2D complex dis-crete assemblies modelled using cracking blocks with non-dilatant interfaces. In: Iványi, P., Kruis, J., Topping, B.H.V. (ed.), Proceedings of the Fifteenth International Conference on Computational Structures Technology, pp. 1–14. Civil-Comp Press (2024)
17. Ramaglia, G., Lignola, G.P., Prota, A.: Collapse analysis of slender masonry barrel vaults. Eng. Struct. **117**, 86–100 (2016)
18. Gilbert, M., Casapulla, C., Ahmed, H.M.: Limit analysis of masonry block structures with non-associative frictional joints using linear programming. Comput. Struct. **84**(13–14), 873–887 (2006)
19. Mousavian, E., Casapulla, C.: Structurally informed design of interlocking block assemblages using limit analysis. J. Comput. Des. Eng. **7**(4), 448–468 (2020)
20. Casapulla, C., Mousavian, E., Argiento, L., Ceraldi, C., Bagi, K.: Torsion-shear behaviour at the interfaces of rigid interlocking blocks in masonry assemblages: experimental investigation and analytical approaches. Mater. Struct. **54**(3) (2021)

21. Casapulla, C., Portioli, F.: Experimental and analytical investigation on the frictional contact behavior of 3D masonry block assemblages. Constr. Build. Mater. **78**, 126–143 (2015)
22. Portioli, F., Casapulla, C., Cascini, L., D'Aniello, M., Landolfo, R.: Limit analysis by linear programming of 3D masonry structures with associative friction laws and torsion interaction effects. Arch. Appl. Mech. **83**, 1415–1438 (2013)